ISSN 1029-9599, Physical Mesomechanics, 2021, Vol. 24, No. 1, pp. 20–31. © Pleiades Publishing, Ltd., 2021.
Russian Text © The Author(s), 2020, published in Fizicheskaya Mezomekhanika, 2020, Vol. 23, No. 4, pp. 31–42.

Method of Images Solution for an Edge Dislocation and a Circular Cavity in Crystalline Solids

K. Nguyen[1]* and A. Mehrabian[1]

[1] *Department of Energy and Mineral Engineering, Earth and Mineral Sciences Energy Institute, The Pennsylvania State University, University Park, PA, 16802 USA*
** e-mail: ktn36@psu.edu*

Received July 15, 2020, revised July 15, 2020, accepted July 31, 2020

Abstract—Mechanics of defects in solids across a wide span of length scales is commonly formulated using the dislocations theory. This paper revisits the classical problem of interaction between an elastic edge dislocation and a circular cavity. A heuristic, yet, mechanistic approach is taken to obtain the stress solution to this problem. The approach uses complex variable theory of elasticity, along with method of images. For this purpose, a definition and formulation of elastic dipole singularities similar to dipole charges in electrostatics is developed. It is shown that an image dislocation with Burger's vector of the same strength as the real dislocation but in opposite direction, as well as a set of four singularities including a dislocation dipole, a moment-dilatation dipole, and two centers of dilatation would establish a circular, traction-free boundary in an infinite elastic medium. Adding a Volterra dislocation to the finite-length edge dislocation from this study would recover the related problem of interaction between an infinite-length edge dislocation and circular cavity. The interesting analogy between the considered elastic problem and the electrostatic problem of interaction between a line electric charge and a cylindrical conductor is discussed.

DOI: 10.1134/S1029959921010045

Keywords: method of images, dislocation, elasticity, mechanics of defects, solid mechanics

NOMENCLATURE

q—magnitude of electrical charge,
q_0—magnitude of image electrical charge,
V—electrical potential,
x—real axis in complex plane, rectangular x coordinate axis,
y—imaginary axis in complex plane, rectangular y coordinate axis,
R_0—a reference radial distance,
R—circular cavity radius centered at the origin,
ξ—the end-coordinate of a finite edge dislocation measured from the origin,
θ—angle measured from x-axis,
G—shear modulus,
ν—Poisson ratio,
σ_{ij}—stress tensor,
∇^2—Laplace operator,
U—Airy's stress function,
z—complex coordinate of physical plane,
Ω—complex stress potential,
ω—complex stress potential,
Re—real part of a complex expression,
Im—imaginary part of a complex expression,
$\mathbf{b}$—Burger's dislocation vector in complex plane,
b_x—glide edge dislocation magnitude,
b_y—climb edge dislocation magnitude,
i—complex unit number, $i = (-1)^{1/2}$,
e—Euler's number, natural logarithm base constant,
ϕ—generic auxiliary potential,
ζ—generic auxiliary location of singularity in complex plane,
J—generic auxiliary magnitude of singularity,
B—auxiliary dislocation magnitude,
Q—auxiliary center of dilatation magnitude,
M—auxiliary moment magnitude,
P—auxiliary combined moment and center of dilatation magnitude,
S—auxiliary coefficient,
||—indicating the norm of a complex expression,
Arg—indicating the argument of a complex expression.

SUBSCRIPT

r—radial direction in cylinder coordinate, centered at the origin,
θ—tangential direction in cylinder coordinate,
i, *j*—stress tensors index,
x—real part of a complex variable,
y—imaginary part of a complex variable,
b—Burger's dislocation vector in complex plane.

SUPERSCRIPT

– —overbar indicating complex conjugate property,
′—derivative in complex plane,
ˆ —dipole of a singularity,
ed—edge dislocation,
dp—dipole of a potential,
fed—indicating a property of a finite length edge dislocation,
V—indicating of the property of a Volterra dislocation.

1. INTRODUCTION

The method of images offers a rather exploratory means of solving certain problems in mathematical physics involving singularities within finite domains, e.g., in electrostatics [1], plane elasticity [2], heat conduction [3], flow of inviscid fluids [4] and theory of vibrations [5]. The technique involves expanding the solution domain to an infinite space by introducing an image of the real problem domain against one or more boundary surfaces or hypersurfaces. Fictitious singularities of deliberately selected strength and location are usually placed in the image domain in such a way that the prescribed boundary conditions of the problem boundary surfaces are secured.

A pioneering application of the images method is found in the [6] on the interaction between point charges and spherical conductors. The two-dimensional variation of the problem is shown in Fig. 1 where a line electric charge q located at $x = \xi$, an image charge $-q$ located at $x = R^2/\xi$, along with an auxiliary

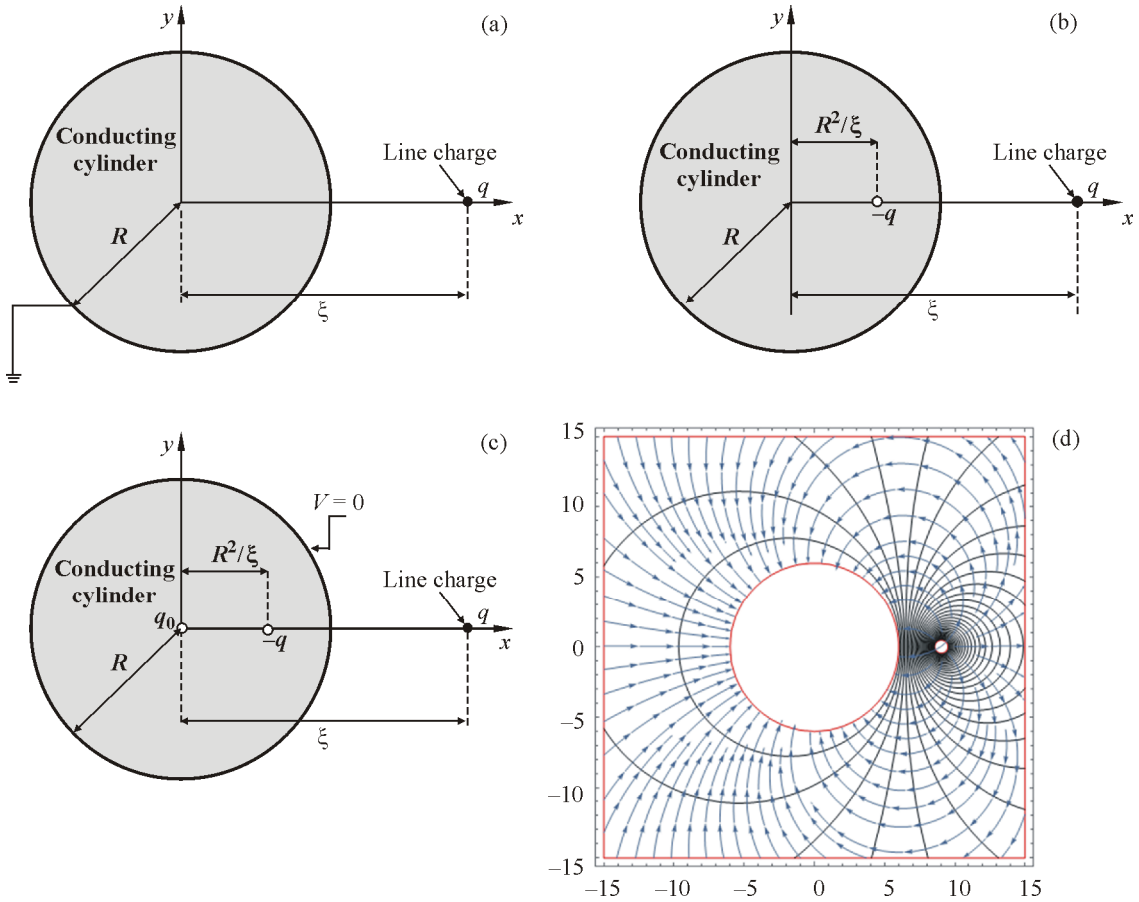

Fig. 1. Schematics of electrostatic problem of a line charge interacting with a conducting cylinder (a), as well as the images charges at image point, $x = R^2/\xi$ (b), and the conductor center, $x = 0$ (c). The arrowed curves and black curves are the resulting electric field and equipotential contours, respectively (d) (color online).

charge of strength $q_0 = -q\ln(R/\xi)\ln^{-1}(R_0/R)$ located at $x = 0$, within an infinite space would produce a circular equipotential contour of radius R centered at the origin of the coordinate system [1]. Thus, the uniqueness theorem of Poisson's equation would immediately establish the solution to the problem of electrostatic interaction between an infinite line charge q located at a distance ξ from the center of a circular conductor held at electric potential $V = 0$ [1].

Method of images has been applied to problems of defects in elastic crystalline solids, in particular, via the theories of dislocations and fracture mechanics. Early contributions to the subject considered the analogy between elastic stress fields of screw dislocations and electrostatic fields of line charges [7, 8]. The interaction between an elastic edge dislocation and a planar boundary at the interface of two dissimilar solids using the images method is presented in [9]. The solutions for the elastic interaction between screw and edge dislocations with boundaries of inhomogeneities were further treated in [10]. Extension of the solution in [7] was later applied to semiconductors technology where the configuration of inhomogeneous strained layer superlattices was shown to allow for filtering screw dislocations in gallium arsenide layers grown on silicon [11]. The phenomenon was reported to be responsible for superior yield strength of lamellar materials compared to the bulk pure crystals of their either constituents. A scaling theory of such strengthening effect based on the method-of-image solution of the repulsive forces between dislocation rows and inhomogeneity interfaces between alternating layers of lamellar materials is given in [12]. More recently, the displacement profile of the interface for the inhomogeneity-dislocation problem was published [13] while multilayer extensions of the solution using successive dislocations images can be found in [14–18]. The method of images has been used to solve for the elastic field of twist disclinations in nonhomogeneous infinite spaces [19] and in hexagonal crystals [20].

A similar record of literature has documented the fundamental and applied solutions on the interaction between dislocations and circular boundaries. Eshelby applied the images method to solve for the problem of a screw dislocation in the vicinity the circular boundary of a thin rod [21]. Recently, the work of Eshelby has been extended to the cases of multiple annular elastic layers [22] and piezoelectric nanowires [23]. The stress field of an edge dislocation in presence of a circular inhomogeneity is somewhat more complex than the alternative problem involving a screw dislocation since the former problem entails biharmonic stress potentials whereas the stress potential of the latter is a harmonic function. The pioneering work by Dundurs and Mura [24] concludes the solution to this problem. The solution in [24] is, however, a pure mathematical guess based on a rather try-and-error investigation of the similarities with the associated stress potentials from the limiting case of two inhomogeneous semi-infinite planes [25, 26]. Dundurs and Mura's solution on the subject was later reformulated in the complex plane [27]. The solution for the case when the circular boundary is coated by a thin layer of different properties is presented in [28] whereas the case of two circular inclusions is treated in [29]. The problem of interaction between an edge dislocation and an elliptic boundary is successfully solved by conformal mapping technique in [30]. The solution for the case of edge dislocation inside an elliptical inclusion is published in [31]. The solution for an edge dislocation interacting with an interfacial crack at the boundary of a circular inhomogeneity is determined in [32]. The case of imperfect boundary interface between the matrix and circular inhomogeneity is investigated in [33]. More recently, the solution to the problem of cavity and dislocation is extended to the case where the matrix is an elastic half-space [34].

This paper uses the electrostatics analogy of images method to revisit and solve the problem of interaction between an edge dislocation and a circular cavity. The nonzero stresses due to the real and image dislocations of opposite sign at the boundary of the cavity are determined and inspected. It is shown that deliberate placement of four auxilliary singularities of determined strength would retrieve traction-free condition of the cavity surface. These mechanical singularities include a dislocation dipole, a moment-dilatation dipole and two centers of dilatation. The strengths of these singularities are obtained from a system of linear algebraic equations that are extracted from the traction-free boundary conditions on the cavity surface. Results are verified by the previous published solution to the same problem [24].

2. THE ELASTIC PROBLEM OF EDGE DISLOCATION AND CIRCULAR CAVITY

Figure 2 illustrates the plane-strain problem where a single edge dislocation of Burger's vector **b** is placed in an infinite elastic medium of elastic constants G, ν located at a distance ξ from the center of a traction-free circular cavity. The problem boundary conditions consist of zero traction on the cavity boundary, i.e.,

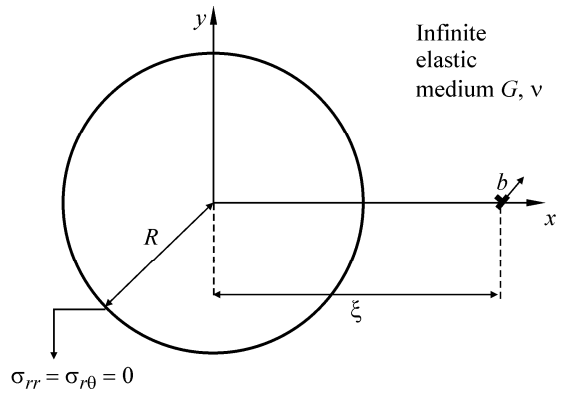

Fig. 2. Schematic of a finite edge dislocation and a circular cavity in an infinite elastic domain.

$$\sigma_{rr}(R,\theta)=0, \tag{1}$$

$$\sigma_{r\theta}(R,\theta)=0 \tag{2}$$

together with zero far-field stresses, as follows:

$$\sigma_{ij}(r\to\infty,\theta)=0. \tag{3}$$

The polar-coordinate form of Navier's equations of static equilibrium, along with stress compatibility condition, takes the following forms [2]:

$$\frac{\partial\sigma_{rr}}{\partial r}+\frac{1}{r}\frac{\partial\sigma_{r\theta}}{\partial\theta}+\frac{\sigma_{rr}-\sigma_{\theta\theta}}{r}=0, \tag{4}$$

$$\frac{1}{r}\frac{\partial\sigma_{\theta\theta}}{\partial\theta}+\frac{\partial\sigma_{r\theta}}{\partial r}+\frac{2\sigma_{r\theta}}{r}=0, \tag{5}$$

$$\nabla^2(\sigma_{rr}+\sigma_{\theta\theta})=0, \tag{6}$$

where $\nabla^2=\frac{\partial}{\partial r}\left(\frac{1}{r}\frac{\partial\sigma}{\partial r}\right)+\frac{1}{r^2}\frac{\partial^2}{\partial\theta^2}$ is Laplacian operator of polar coordinate.

The stress components can be given in terms of Airy stress function $U(r,\theta)$ [35]:

$$\sigma_r=\frac{1}{r}\frac{\partial U}{\partial r}+\frac{1}{r^2}\frac{\partial^2 U}{\partial\theta^2}, \tag{7}$$

$$\sigma_\theta=\frac{\partial^2 U}{\partial r^2}, \tag{8}$$

$$\tau_{r\theta}=-\frac{\partial}{\partial r}\left(\frac{1}{r}\frac{\partial U}{\partial\theta}\right). \tag{9}$$

Direct substitution of the Eqs. (7)–(9) would verify that Airy's stress function satisfies both the stress equilibrium and compatibility conditions expressed in Eqs. (4)–(6), provided that $U(r,\theta)$ is a biharmonic function, i.e., $\nabla^2(\nabla^2 U)=0$.

The Airy stress U can be written in terms of two constitutive complex potential functions $\Omega(z)$ and $\omega(z)$, as follows [36]:

$$U(r,\theta)=1/2[\bar{z}\Omega(z)+z\bar{\Omega}(z)+\omega(z)+\bar{\omega}(z)], \tag{10}$$

where the in-plane stresses can be expressed as a combination of these two complex potentials as

$$\sigma_{rr}+\sigma_{\theta\theta}=2[\Omega'(z)+\bar{\Omega}'(z)], \tag{11}$$

$$\sigma_{\theta\theta}-\sigma_{rr}+2i\sigma_{r\theta}=2\frac{z}{\bar{z}}[\bar{z}\Omega''(z)+\omega''(z)], \tag{12}$$

$$\sigma_{rr}-i\sigma_{r\theta}=\Omega'(z)+\bar{\Omega}'(z)-\frac{z}{\bar{z}}[\bar{z}\Omega''(z)+\omega''(z)]. \tag{13}$$

In polar coordinate, the in-plane stresses are calculated from Eqs. (11)–(13), as follows:

$$\sigma_{rr}(r,\theta)=\mathrm{Re}\left[2\Omega'(z)-z\Omega''(z)-\frac{z}{\bar{z}}\omega''(z)\right], \tag{14}$$

$$\sigma_{\theta\theta}(r,\theta)=\mathrm{Re}\left[2\Omega'(z)+z\Omega''(z)+\frac{z}{\bar{z}}\omega''(z)\right], \tag{15}$$

$$\sigma_{r\theta}(r,\theta)=\mathrm{Im}\left[z\Omega''(z)+\frac{z}{\bar{z}}\omega''(z)\right]. \tag{16}$$

2.1. Method of Images Solution

Without loss of generality, the real axis of the complex plane with the origin at the center of the cavity in Fig. 2 is assumed to align with the line connecting the dislocation and cavity center. For a dislocation with Burger's vector **b** located at $z=\xi$ in an infinite elastic field, the complex potential functions take on the following form [36, 37]:

$$\Omega_{\mathbf{b}}^{\mathrm{ed}}(z,\xi)=\frac{G\mathbf{b}}{4\pi i(1-\nu)}\ln(z-\xi), \tag{17}$$

$$\omega_{\mathbf{b}}'^{\mathrm{ed}}(z,\xi)=\frac{G}{4\pi i(1-\nu)}\left[-\bar{\mathbf{b}}\ln(z-\xi)-\frac{b\bar{\xi}}{z-\xi}\right]. \tag{18}$$

Kelvin's method of images [6] for circular boundaries is followed by placing an image edge dislocation with Burger's vector $-\mathbf{b}$ at $z=R^2/\xi$. This method follows a direct analogy of the well-known electrostatics solution for interaction between a line charge and a circular conductor, as shown in Fig. 1. The complex potential functions pertaining to the real dislocation at $z=\xi$ and image dislocation at $z=R^2/\xi$ are written as

$$\Omega(z,\xi)=\Omega_{\mathbf{b}}^{\mathrm{ed}}(z,\xi)+\Omega_{-\mathbf{b}}^{\mathrm{ed}}\left(z,\frac{R^2}{\xi}\right), \tag{19}$$

$$\omega'(z,\xi)=\omega_{\mathbf{b}}'^{\mathrm{ed}}(z,\xi)+\omega_{-\mathbf{b}}'^{\mathrm{ed}}\left(z,\frac{R^2}{\xi}\right), \tag{20}$$

where Ω^{ed} and ω'^{ed} are defined in Eqs. (17) and (18). By substituting Eqs. (19) and (20) in Eq. (13), the in-plane shear and radial stresses at the hole's boundary $z=Re^{i\theta}$ simplify to

$$\sigma_{rr} - i\sigma_{r\theta} = \frac{G\mathbf{b}}{4\pi i(1-\nu)}\left[\frac{1}{Re^{i\theta}-\xi} - \frac{1}{Re^{i\theta}-R^2/\xi} + \frac{Re^{i\theta}}{(Re^{i\theta}-\xi)^2} - \frac{Re^{i\theta}}{(Re^{i\theta}-R^2/\xi)^2}\right] - \frac{G\bar{\mathbf{b}}}{4\pi i(1-\nu)}\left[\frac{1}{Re^{-i\theta}-\xi} - \frac{1}{Re^{-i\theta}-R^2/\xi}\right] - \frac{Ge^{2i\theta}}{4\pi i(1-\nu)}\left[\frac{\mathbf{b}\xi}{(Re^{i\theta}-\xi)^2} - \frac{\mathbf{b}R^2}{\xi(Re^{i\theta}-R^2/\xi)^2} + \frac{\bar{\mathbf{b}}}{Re^{i\theta}-R^2/\xi} - \frac{\bar{\mathbf{b}}}{Re^{i\theta}-\xi}\right]. \quad (21)$$

The correct solution to the considered problem requires the right side of Eq. (21) to vanish. Hence, the task at hand becomes a search for supplementary singularities negating the right side of Eq. (21).

The mathematical form of stresses expression in Eq. (21) suggests an ad hoc method to secure this condition. It appears that singularities of higher order can be used for this purpose. Dipoles of elastic singularities could form the basis of a plausible solution. Appendix A presents a formulation for potential functions of the elastic dipoles, as well as the corresponding formulae for known elastic singularities including dislocations, moments, or centers of dilatation. The generalized formulations of singularities are summarized in Tables A1 and A2. In particular, from Appendix A, the complex potentials of a dislocation dipole with Burgers vector $\hat{B}_1$ at R^2/ξ are given by substituting Eqs. (17) and (18) in Eq. (A1):

$$\Omega^{\mathrm{dp}}_{\hat{B}_1}\left(z, \frac{R^2}{\xi}\right) = -\frac{G\hat{B}_1}{4\pi i(1-\nu)}\frac{1}{z-R^2/\xi}, \quad (22)$$

$$\omega'^{\mathrm{dp}}_{\hat{B}_1}\left(z, \frac{R^2}{\xi}\right) = \frac{G}{4\pi i(1-\nu)} \times\left(\bar{\hat{B}}_1\frac{1}{z-R^2/\xi} - \frac{\hat{B}_1}{z-R^2/\xi} - \frac{\hat{B}_1 R^2/\xi}{(z-R^2/\xi)^2}\right), \quad (23)$$

where $\hat{B}_1$ is the unknown Burgers vector of the dislocation dipole at the image point. An attempt by introducing a dislocation dipole into Eq. (21) reveals that it is impossible to completely negate the nonzero terms on the right side of Eq. (21) with a dislocation dipole alone. Thus, auxiliary complex potentials that, likewise, contain second order singularity originating from a combined moment-center of dilatation at the image location are used as well. From Eqs. (A8) and (A9), the potential functions pertaining to a combined singularity of the form $P_1 = M_1 + iQ_1$ located at R^2/ξ in a complex plane, would find the following form:

$$\Omega_{P_1}\left(z, \frac{R^2}{\xi}\right) = 0, \quad (24)$$

$$\omega'_{P_1}\left(z, \frac{R^2}{\xi}\right) = \frac{G}{4\pi i(1-\nu)}\frac{P_1}{z-R^2/\xi}, \quad (25)$$

where P_1 is the complex variable of the combined singularity, M_1 and Q_1 are real-valued magnitude of moment and center of dilatation at the image location. $P_1 = -P(1-\nu)/G$ is defined to maintain the consistency with the generic definition in Appendix A. Appendix B shows that dislocation dipole $\hat{B}_1$ induces third order singularity to the problem, which by itself does not cancel out with any other terms. As a result, a combined moment-center of dilatation dipole is also placed at the image location, whose magnitude $\hat{P}_2$ is determined in such a way to reduce the third order singularity arising from the previously selected dislocation dipole. Following the derivations in Appendix B, $\hat{P}_2$ and $\hat{B}_1$ are related by

$$\hat{P}_2 = \hat{B}_1(R^2 - \xi^2)/\xi. \quad (26)$$

By adding the combined moment-center of dilatation dipole $\hat{P}_2$ and by substituting Eq. (26) into the total potential, the zero in-plane shear stress at the circular cavity's wall suggests an approach to determine the magnitude of $\hat{B}_1$ and P_1. Since $\hat{B}_1$ and P_1 are complex variables, they can be written as $\hat{B}_1 = \hat{B}_{1x} + i\hat{B}_{1y}$ and $P_1 = M_1 + iQ_1$. Thus, the complex expanded form of Eq. (16) determines the shear stress around the circular hole containing the physical and image dislocations, one dislocation dipole $\hat{B}_1$, one moment-center of dilatation dipole $\hat{P}_2$ and one moment-center of dilatation P_1. The resulting mathematical expression would find the following form:

$$\sigma_{r\theta}(z = Re^{i\theta}) = -\frac{G}{4\pi(1-\nu)R^3(R^2+\xi^2-2R\xi\cos\theta)^2} \times[4b_xR^5\xi - 4b_xR^3\xi^3 - 4\hat{B}_{1x}R\xi^4 - M_1R\xi^4 + 2(b_x(-R^6+R^2\xi^4) + \xi^3(M_1R^2 + \hat{B}_{1x}(R^2+\xi^2)))\cos\theta - M_1R^3\xi^2\cos(2\theta) + \sin\theta(-2b_yR^6 + 2\hat{B}_{1y}R^2\xi^3 - 2Q_1R^2\xi^3 + 2b_yR^2\xi^4 + 2\hat{B}_{1y}\xi^5) + \sin(2\theta)(2b_yR^5\xi - 2\hat{B}_{1y}R^3\xi^2 + Q_1R^3\xi^2 - 2b_yR^3\xi^3)]. \quad (27)$$

The vanishing shear stress condition at the interface demands that all groups of trigonometric functions should identically vanish. The resulting set of linear algebraic equations is outlined, as follows:

$$\begin{gathered} M_1 R^3 \xi^2 = 0, \\ 4b_x R^5 \xi - 4b_x R^3 \xi^3 - 4\hat{B}_{1x} R \xi^4 - M_1 R \xi^4 = 0, \\ b_x(-R^6 + R^2\xi^4) + \xi^3(M_1 R^2 + \hat{B}_{1x}(R^2 + \xi^2)) = 0, \\ -2b_y R^6 + 2\hat{B}_{1y} R^2 \xi^3 - 2Q_1 R^2 \xi^3 \\ + 2b_y R^2 \xi^4 + 2\hat{B}_{1x} \xi^5 = 0, \\ 2b_y R^5 \xi - 2\hat{B}_{1y} R^3 \xi^2 + Q_1 R^3 \xi^2 - 2b_y R^3 \xi^3 = 0. \end{gathered} \tag{28}$$

Equations (28) constitute a set of 5 linear algebraic equations to be solved for only 4 variables. Although there are more equations than variables, the solution can be uniquely determined, as follows:

$$\begin{gathered} \hat{B}_1 = -\frac{R^2(\xi^2 - R^2)}{\xi^3}\bar{\mathbf{b}}, \\ \hat{P}_2 = \frac{R^2(R^2 - \xi^2)^2}{\xi^4}\bar{\mathbf{b}}, M_1 = 0, \\ Q_1 = 2\,\mathrm{Im}[\mathbf{b}]\frac{\xi^4 - R^4}{\xi^3}. \end{gathered} \tag{29}$$

Although the in-plane shear stress condition in Eq. (2) is met, the radial stress at the boundary is yet to be satisfied. The residual radial stress at the wall's boundary after $\hat{B}_1, \hat{P}_2$ and P_1 having been determined is

$$\sigma_{rr}(z = R e^{i\theta}) = \frac{2b_y G(\xi^2 - R^2)}{4\pi(1-\nu)R^2\xi}. \tag{30}$$

The constant residual radial stress in the elastic problem is similar to the electrostatic subproblem in Fig. 1b where a constant potential is found on the interface of a conducting cylinder. Thus from Eq. (30) it is straight-forward to include a uniquely defined center of dilatation at the cavity center to negate the obtained radial stress. From Appendix A, the complex potential of a dilatation of magnitude Q_3 at the cavity center is found by

$$\Omega_{Q_3}(z, 0) = 0, \tag{31}$$

$$\omega'_{Q_3}(z, 0) = \frac{G}{4\pi(1-\nu)R^2\xi}\frac{Q_3}{z}, \tag{32}$$

where Q_3 is the strength of dilatation center at the origin. Using (14), (30) and (32), Q_3 is determined as

$$Q_3 = -2\,\mathrm{Im}[\mathbf{b}]\frac{\xi^2 - R^2}{\xi}. \tag{33}$$

3. DISCUSSION

In summary, the exact analytical solution of the problem of a single dislocation **b** placed at an arbitrary distance ξ away from the center of circular hole can be decomposed into two subproblems in an infinite continuum domain: (i) the dislocation **b** at ξ and (ii) complementary terms to account for the stress free boundary condition at the cavity boundary. The latter second problem can be further written as a superposition of five singularities in infinite elastic domain. Figure 3 illustrates the summary of these elastic singularities.

Consequently, the complex holomorphic functions describing the interaction of a dislocation of finite length $(\xi - R)$ with the circular cavity are obtained, as follows:

$$\Omega(z, \xi) = \Omega_{\mathbf{b}}^{\mathrm{ed}}(z, \xi) + \Omega_{-\mathbf{b}}^{\mathrm{ed}}\left(z, \frac{R^2}{\xi}\right) + \Omega_0(z), \tag{34}$$

$$\begin{aligned} \omega'(z, \xi) = \omega'^{\mathrm{ed}}_{\mathbf{b}}(z, \xi) + \omega'^{\mathrm{ed}}_{-\mathbf{b}}\left(z, \frac{R^2}{\xi}\right) \\ + \omega'_0(z) + \omega'_1(z), \end{aligned} \tag{35}$$

where the generic primary complex potentials of a dislocation in an infinite elastic field $\Omega_{\mathbf{b}}^{\mathrm{ed}}(z, \xi)$, $\Omega_{-\mathbf{b}}^{\mathrm{ed}}(z, R^2/\xi)$, $\omega'^{\mathrm{ed}}_{\mathbf{b}}(z, \xi)$, and $\omega'^{\mathrm{ed}}_{-\mathbf{b}}(z, R^2/\xi)$ are obtained from Eqs. (14) and (15), $\Omega_0(z)$, $\omega'_0(z)$ and $\omega'_1(z)$ are extra singular expressions due to the center of dilation and moment-dilatation dipole at the image point, as well as the center of dilatation at the cavity center. These potentials are obtained as

$$\Omega_0(z) = \frac{G\bar{\mathbf{b}}}{4\pi i(1-\nu)}\frac{R^2(\xi^2 - R^2)}{\xi^3(z - R^2/\xi)}, \tag{36}$$

$$\omega'_0(z) = \frac{G\bar{\mathbf{b}}}{4\pi i(1-\nu)}\frac{R^2(\xi^2 - R^2)}{\xi^2(z - R^2/\xi)^2}, \tag{37}$$

$$\omega'_1(z) = \frac{G\,\mathrm{Im}[\mathbf{b}]}{4\pi(1-\nu)}\frac{2(\xi^2 - R^2)}{\xi}\left(\frac{1}{z - R^2/\xi} - \frac{1}{z}\right). \tag{38}$$

Table 1 shows the striking analogy between the electrostatic and elastostatic problems. The associated method-of-images solutions to both problems involve placing an image singularity at $z = R^2/\xi$, as well as an auxiliary singularity at the cavity center. However, a set of three extra auxiliary singularities at the image location is required in the case of the elastostatic problem to reproduce the traction-free boundary conditions on the cavity.

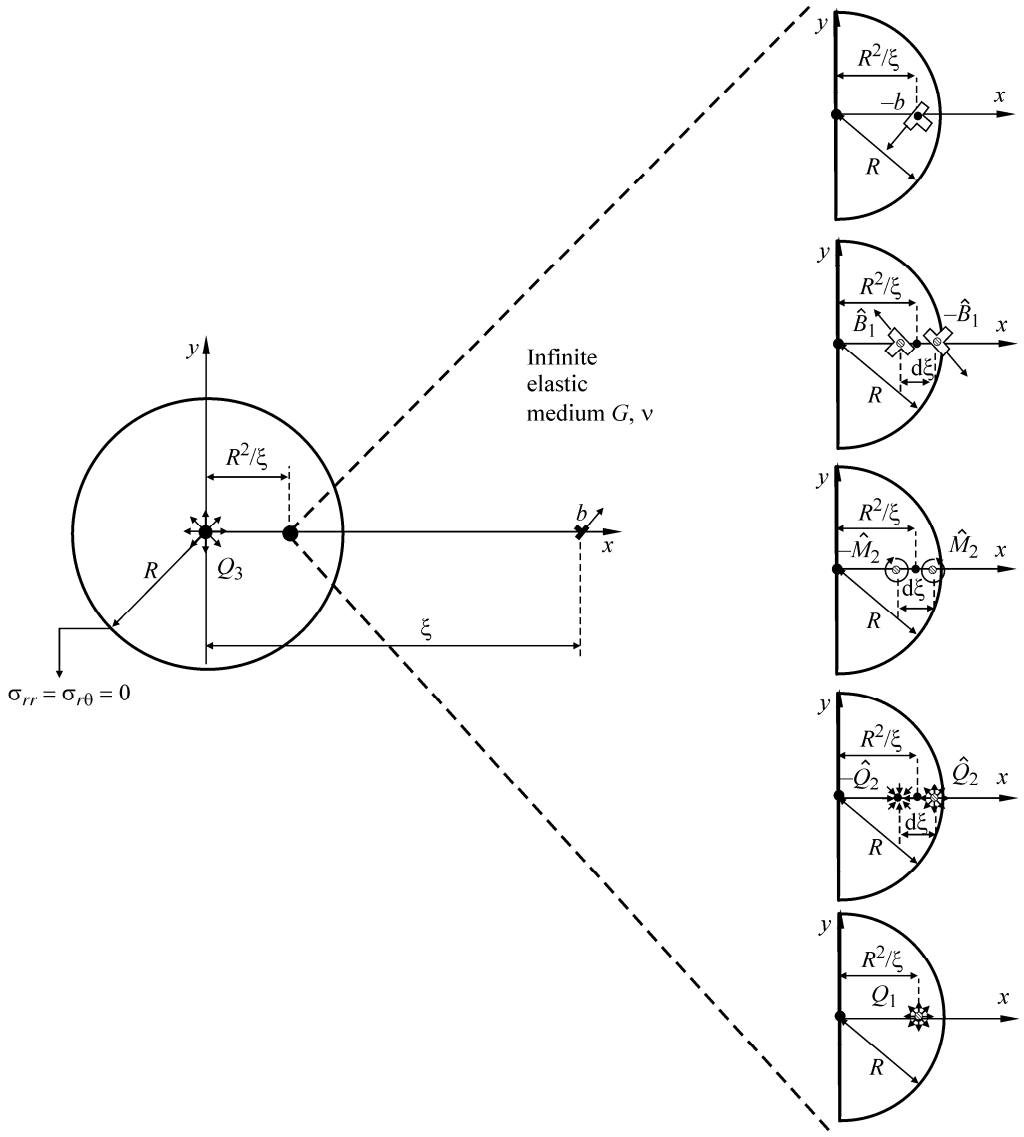

Fig. 3. Schematics of the method-of-images solution to the dislocation and cavity problem in an infinite elastic domain.

3.1. Verification with Results of [24]

From Eqs. (34) to (38), Airy stress functions pertaining to glide b_x and climb b_y components of the edge dislocation $\mathbf{b} = b_x + ib_y$ in presence of a circular cavity can be derived by using Eq. (10). The results are expressed as

$$U_x = \frac{G_1 b_x}{4\pi(1-\nu_1)}\left\{-2\,|\,z-\xi\,|\ln|\,z-\xi\,|\sin\left(\mathrm{Arg}(z-\xi)\right)\right.$$
$$+2\left|z-\frac{R^2}{\xi}\right|\ln\left|z-\frac{R^2}{\xi}\right|\sin\left[\mathrm{Arg}\left(z-\frac{R^2}{\xi}\right)\right]$$
$$-\frac{(\xi^2-R^2)R^2}{\xi^3}\left(\sin\left[2\mathrm{Arg}\left(z-\frac{R^2}{\xi}\right)\right]\right.$$
$$\left.\left.-\frac{\xi^2-R^2}{\xi}\frac{\sin\left[\mathrm{Arg}(z-R^2/\xi)\right]}{\left|z-R^2/\xi\right|}\right)\right\}, \qquad (39)$$

$$U_y = \frac{G_1 b_y}{4\pi(1-\nu_1)}\left\{2\,|\,z-\xi\,|\ln|\,z-\xi\,|\cos(\mathrm{Arg}(z-\xi))\right.$$
$$-2\left|z-\frac{R^2}{\xi}\right|\ln\left|z-\frac{R^2}{\xi}\right|\cos\left[\mathrm{Arg}\left(z-\frac{R^2}{\xi}\right)\right]$$
$$+\frac{(\xi^2-R^2)R^2}{\xi^3}\left(\frac{2\xi^2}{R^2}\ln\left|z-\frac{R^2}{\xi}\right|\right.$$
$$\left.\left.-\cos\left[2\mathrm{Arg}\left(z-\frac{R^2}{\xi}\right)\right]+\frac{\xi^2-R^2}{\xi}\right.\right.$$

Table 1. The analogy between method-of-images solutions of the electrostatic and elastostatic problems with circular boundaries

	Electrostatics		Elastostatics	
Potential function	$\nabla^2 V = 0$		$\nabla^2(\nabla^2 \mathrm{U}) = 0$	
Boundary conditions at $z = Re^{i\theta}$	$V = 0$		$\frac{\partial}{\partial r}\left(\frac{1}{r}\frac{\partial \mathrm{U}}{\partial \theta}\right) = 0, \frac{1}{r}\frac{\partial \mathrm{U}}{\partial r} + \frac{1}{r^2}\frac{\partial^2 \mathrm{U}}{\partial \theta^2} = 0$	
Singularity location	Description	Magnitude	Description	Magnitude
Singularity at $z = \xi$	Electric charge	q	Dislocation	$\mathbf{b}$
Primary image singularity at $z = R^2/\xi$	Image electric charge	$-q$	Image dislocation	$-\mathbf{b}$
Auxiliary singularities at $z = R^2/\xi$	None	0	Dislocation dipole	$-\frac{R^2(\xi^2 - R^2)}{\xi^3}\bar{\mathbf{b}}$
			Moment-dilatation dipole	$\frac{\bar{\mathbf{b}}R^2(\xi^2 - R^2)^2}{\xi^4}$
			Center of dilatation	$\frac{2\,\mathrm{Im}(\mathbf{b})(\xi^4 - R^4)}{\xi^3}$
Auxiliary singularities at $z = 0$	Electric charge	$-\frac{q\ln(R/\xi)}{\ln(R_0/R)}$	Center of dilatation	$-\frac{2\,\mathrm{Im}(\mathbf{b})(\xi^2 - R^2)}{\xi}$

$$\times \frac{\cos\left[\mathrm{Arg}(z - R^2/\xi)\right]}{\left|z - R^2/\xi\right|}\Bigg) - 2\frac{\xi^2 - R^2}{\xi}\ln|z|\Bigg\}. \quad (40)$$

The infinite edge dislocation from Dundurs and Mura's formulation [24] can be retrieved from the finite-length edge dislocation solution of this study if Eqs. (39) and (40) are superposed with a Volterra dislocation [5], whose potentials are written as

$$\Omega_{\mathbf{b}}^{\mathrm{V}}(z) = \frac{G\mathbf{b}}{4\pi i(1-\nu)}\ln z, \quad (41)$$

$$\omega_{\mathbf{b}}'^{\mathrm{V}}(z) = -\frac{G}{4\pi i(1-\nu)}\left[\bar{\mathbf{b}}(\ln z + 1) + \frac{bR^2}{z^2}\right]. \quad (42)$$

Hence, the Airy stress of the Volterra dislocation becomes:

$$\mathrm{U}_{\mathbf{b}}^{\mathrm{V}}(z) = \mathrm{Re}\left[-\frac{\bar{\mathbf{b}}}{i}z(\overline{\ln z} + \ln z) + \frac{\mathbf{b}}{i}\frac{R^2}{z}\right]. \quad (43)$$

Equation (43) pertains to the special case of a more generalized Volterra dislocation in Eq. (44) of a ring-shaped elastic field given by Lardner [38], whose schematic is displayed in Fig. 4:

$$\mathrm{U}_{\mathbf{b}}^{\mathrm{V}}(z) = \mathrm{Re}\left[-\frac{\bar{\mathbf{b}}}{i}z(\overline{\ln z} + \ln z) + \frac{\bar{\mathbf{b}}}{i}\frac{z^2\bar{z}}{R_1^2} + \frac{\mathbf{b}}{i}\frac{R^2}{z}\right]. \quad (44)$$

It is easy to see that as $R_1 \to \infty$, the limiting case from Eq. (44) will be simplified into Eq. (43). Superposing Volterra's dislocation stress function by Eq. (43) on the glide and climb components of the Burger's vector b_x and b_y with potentials $\Omega(z)$ and $\omega'(z)$ defined by Eqs. (34)–(38) and rederiving the real-valued Airy stress function from Eq. (10), the following identical formulation of Dundurs and Mura for an infinite-length dislocation is recovered [24]:

$$\mathrm{U}_x = \frac{G_1 b_x}{4\pi(1-\nu_1)}\Big\{-2r_1\ln r_1\sin\theta_1 + 2(r_2\ln r_2\sin\theta_2 - r\ln r\sin\theta)$$

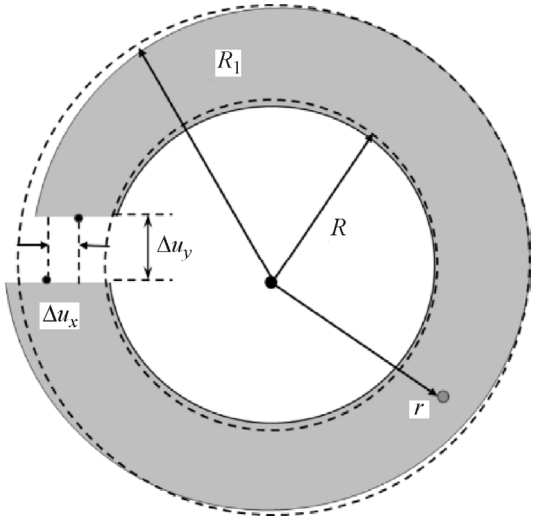

Fig. 4. Schematics of a ring-shaped Volterra dislocation.

$$-\frac{(\xi^2-R^2)R^2}{\xi^3}\left[\sin(2\theta_2)\right.$$
$$\left.-\frac{(\xi^2-R^2)}{\xi}\frac{\sin\theta_2}{r_2}\right]-R^2\frac{\sin\theta}{r}\Bigg\}.$$
$$U_y=\frac{G_1 b_y}{4\pi(1-\nu_1)}\Bigg\{2r_1\ln r_1\cos\theta_1$$
$$-2(r_2\ln r_2\sin\theta_2-r\ln r\cos\theta)$$
$$+\frac{(\xi^2-R^2)R^2}{\xi^3}\left[\frac{2\xi^2}{R^2}\ln r_2\right. \qquad (45)$$
$$\left.-\cos(2\theta_2)+\frac{(\xi^2-R^2)}{\xi}\frac{\cos\theta_2}{r_2}\right]$$
$$-2\frac{(\xi^2-R^2)}{\xi}\ln r+R^2\frac{\cos\theta}{r}\Bigg\},\ r=|z|,$$
$$r_1=|z-\xi|,\ r=|z|,$$
$$r_2=\left|z-\frac{R^2}{\xi}\right|,$$
$$\theta_1=\mathrm{Arg}(z-\xi),$$
$$\theta_2=\mathrm{Arg}\left(z-\frac{R^2}{\xi}\right),$$
$$\theta=\mathrm{Arg}(z).$$

4. CONCLUSION

Method of images is used to solve the problem of a circular cavity interacting with a finite edge dislocation. It is shown that aside from the image dislocation, a set of three singularities including a center of dilatation, a moment dilatation dipole and a dislocation dipole at the image point, as well as a center of dilation at the cavity center, would secure the traction-free boundary of the cavity. The presented solution closely mimics Kelvin's solution of interacting line charges and cylindrical conductors in electrostatics.

APPENDIX A. DIPOLES OF ELASTIC SINGULARITIES

The complex potential of dipole of strength $\hat{J}$ is, defined by a pair of corresponding singularities, with the same magnitude of strength J but in opposite in direction, one located at an arbitrary point ζ and the other located at an infinitesimal distance $\zeta+\mathrm{d}\zeta$ in such a way that $\hat{J}=J\mathrm{d}\zeta$ is a finite value [39, 40]. With this definition, supposing the potential function $\phi(z,\zeta)$ with singularity's magnitude J, the complex potentials of a dipole can then be obtained, as follows:

$$\phi_{\hat{J}}^{\mathrm{dp}}(z,\zeta)=\lim_{\mathrm{d}\zeta\to 0}\left(\phi_J(z,\zeta)+\phi_{-J}(z,\zeta+\mathrm{d}\zeta)\right)$$
$$=J\left(\frac{\partial}{\partial\zeta}[\phi(z,\zeta)]\right)\mathrm{d}\zeta=\hat{J}\frac{\partial}{\partial\zeta}[\phi(z,\zeta)]. \qquad (A1)$$

Similar to the electrostatic charge dipoles, neither J nor $\mathrm{d}\zeta$ would have any physical meaning since the former tends to infinity while the latter is infinitesimally small. In this context, the dipole's magnitude is written in terms of $\hat{J}$, which has a finite magnitude. Hence, from Eqs. (17), (18) and (A1) the dipole of a dislocation, whose magnitude at ζ is the Burgers' vector $\hat{B}$, becomes:

$$\Omega_{\hat{B}}^{\mathrm{dp}}(z,\zeta)=-\frac{G\hat{B}}{4\pi i(1-\nu)}\frac{1}{z-\zeta}, \qquad (A2)$$

$$\omega_{\hat{B}}^{\prime\mathrm{dp}}(z,\zeta)=\frac{G}{4\pi i(1-\nu)}\left[\frac{\bar{\hat{B}}}{z-\zeta}-\frac{\hat{B}}{z-\zeta}-\frac{\hat{B}\zeta}{(z-\zeta)^2}\right]. \qquad (A3)$$

The complex potential of a moment and a center of dilatation are outlined in Eqs. (A4), (A5) and (A6), (A7), respectively [41]:

$$\Omega_M(z,\zeta)=0, \qquad (A4)$$

$$\omega_M'(z,\zeta)=\frac{iM}{4\pi}\frac{1}{z-\zeta}, \qquad (A5)$$

$$\Omega_Q(z,\zeta)=0, \qquad (A6)$$

$$\omega_Q'(z,\zeta)=-\frac{Q}{4\pi}\frac{1}{z-\zeta}, \qquad (A7)$$

where M and Q are real-valued magnitude of a moment and a center of dilatation, respectively. Since their forms are identical with the same order of singularity at point ζ, it is convenient to define a complex variable combining moments and centers of dilatation together, denoted as $P=M+iQ$. Thus, with this definition, the combined complex potential becomes:

Table A1. Complex potential $\Omega(z,\zeta)$

	$\ln(z-\zeta)$	$1/(z-\zeta)$
Dislocation B	$\frac{GB}{4\pi i(1-\nu)}$	0
Moment M	0	0
Center of dilatation Q	0	0
Dislocation dipole $\hat{B}$	0	$-\frac{G\hat{B}}{4\pi i(1-\nu)}$
Moment dipole $\hat{M}$	0	0
Center of dilatation dipole $\hat{Q}$	0	0

$$\Omega_P(z,\zeta)=0, \tag{A8}$$

$$\omega'_P(z,\zeta)=\frac{iP}{4\pi}\frac{1}{z-\zeta}. \tag{A9}$$

Using the definition of dipoles (A1), a combined moment-center of dilatation dipole of magnitude $\hat{P}=\hat{M}+i\hat{Q}$ located at ζ in a two-dimensional plane is defined by the potentials:

$$\Omega^{\mathrm{dp}}_{\hat{P}}(z,\zeta)=0, \tag{A10}$$

$$\omega'^{\mathrm{dp}}_{\hat{P}}(z,\zeta)=\frac{i\hat{P}}{4\pi}\frac{1}{(z-\zeta)^2}. \tag{A11}$$

A summary of singularities and their associated potentials is tabulated in Tables A1 and A2.

APPENDIX B. REDUCTION OF THE THIRD-ORDER SINGULARITY

Adding a dislocation dipole $\hat{B}_1$ and a combined moment-center of dilatation P_1 to Eq. (21), the boundary stress terms, i.e., $z=Re^{i\theta}$ would find the following form

$$\sigma_{rr}-i\sigma_{r\theta}=\frac{G}{4\pi i(1-\nu)}\left(\frac{b}{Re^{i\theta}-\xi}-\frac{b}{Re^{i\theta}-R^2/\xi}+\frac{\hat{B}_1}{(Re^{i\theta}-R^2/\xi)^2}+\frac{bRe^{i\theta}}{(Re^{i\theta}-\xi)^2}-\frac{bRe^{i\theta}}{(Re^{i\theta}-R^2/\xi)^2}+\frac{2Re^{i\theta}\hat{B}_1}{(Re^{i\theta}-R^2/\xi)^3}\right)-\frac{G}{4\pi i(1-\nu)}$$

Table A2. Complex potential $\omega'(z,\ \zeta)$

	$\ln(z-\zeta)$	$1/(z-\zeta)$	$1/(z-\zeta)^2$
Dislocation B	$-\frac{G\bar{B}}{4\pi i(1-\nu)}$	$-\frac{GB}{4\pi i(1-\nu)}$	0
Moment M	0	$\frac{iM}{4\pi}$	0
Center of dilatation Q	0	$-\frac{Q}{4\pi}$	0
Dislocation dipole $\hat{B}$	0	$\frac{G(\bar{\hat{B}}-\hat{B})}{4\pi i(1-\nu)}$	$-\frac{G\hat{B}}{4\pi i(1-\nu)}$
Moment dipole $\hat{M}$	0	0	$\frac{i\hat{M}}{4\pi}$
Center of dilatation dipole $\hat{Q}$	0	0	$-\frac{\hat{Q}}{4\pi}$

$$\times\left(\frac{\bar{\mathbf{b}}}{Re^{-i\theta}-\xi}-\frac{\bar{\mathbf{b}}}{Re^{-i\theta}-R^2/\xi}+\frac{\bar{\hat{B}}_1}{(Re^{-i\theta}-R^2/\xi)^2}\right)-\frac{Ge^{2i\theta}}{4\pi i(1-\nu)}\left(\frac{\mathbf{b}\xi}{(Re^{i\theta}-\xi)^2}-\frac{\mathbf{b}R^2}{\xi(Re^{i\theta}-R^2/\xi)^2}+\frac{\bar{\mathbf{b}}}{Re^{i\theta}-R^2/\xi}-\frac{\bar{\mathbf{b}}}{Re^{i\theta}-\xi}+\frac{\hat{B}_1}{(Re^{i\theta}-R^2/\xi)^2}-\frac{\bar{\hat{B}}_1}{(Re^{i\theta}-R^2/\xi)^2}+\frac{2\hat{B}_1R^2}{\xi(Re^{i\theta}-R^2/\xi)^3}-\frac{P_1}{(Re^{i\theta}-R^2/\xi)^2}\right). \tag{B1}$$

Equation (B1) shows that the dislocation dipole at the image point induces stress singularity of third order. Thus, to negate this third order singularity, a combined moment-center of dilatation dipole is placed at the image point location R^2/ξ so that it is reduced to the second order. To be consistent with the notations of Appendix A, the combined potential magnitude is equivalent to $\hat{P}_2=-(1-\nu)/G\hat{P}$:

$$\Omega^{\mathrm{dp}}_{\hat{P}_2}\left(z,\frac{R^2}{\xi}\right)=0, \tag{B2}$$

$$\omega'^{\mathrm{dp}}_{\hat{P}_2}\left(z,\frac{R^2}{\xi}\right)=\frac{G}{4\pi i(1-\nu)}\frac{\hat{P}_2}{(z-R^2/\xi)^2}, \tag{B3}$$

where $\hat{P}_2=\hat{M}_2+i\hat{Q}_2$ is the complex coefficient of the moment-center of dilatation dipole at the image point. Adding only the third order singularities of stresses induced by dislocation dipole $\hat{B}_1$ and the combined moment-center of dilatation dipole $\hat{P}_2$, the relationship between their magnitudes is determined from substitute into latter part of Eq. (13) at the circular cavity's boundary, i.e.

$$\frac{z}{\bar{z}}[\bar{z}\Omega''(z)+\omega''(z)]_{(z=Re^{i\theta})}=\frac{G}{4\pi i(1-\nu)}\left(\frac{2Re^{i\theta}\hat{B}_1}{(Re^{i\theta}-R^2/\xi)^3}-\frac{2R^2e^{2i\theta}\hat{B}_1}{\xi(Re^{i\theta}-R^2/\xi)^3}+\frac{2e^{2i\theta}\hat{P}_2}{(Re^{i\theta}-R^2/\xi)^3}\right)=-\frac{G2e^{i\theta}}{4\pi i(1-\nu)}\frac{\hat{B}_1(R^2e^{i\theta}-R\xi)-\xi e^{i\theta}\hat{P}_2}{\xi(Re^{i\theta}-R^2/\xi)^3}. \tag{B4}$$

To reduce the third order singularity to second order, the numerator must reduce to a common factor of $(Re^{i\theta}-R^2/\xi)$, hence:

$$\hat{B}_1(R^2e^{i\theta} - R\xi) - \xi e^{i\theta}\hat{P}_2 = S\left(Re^{i\theta} - \frac{R^2}{\xi}\right), \quad \text{(B5)}$$

where S is any linear combination of products containing powers of $e^{i\theta}$, R and ξ. Then, $\hat{P}_2$ is related to $\hat{B}_1$ as

$$\hat{P}_2 = \hat{B}_1\frac{R^2 - \xi^2}{\xi}. \quad \text{(B6)}$$

REFERENCES

1. Jackson, J.D., *Classical Electrodynamics*, John Wiley and Sons, 2007.
2. Barber, J.R., *Elasticity*, Dordrecht: Kluwer Academic Publishers, 2002.
3. Carslaw, H.S. and Jaeger, J.C., *Conduction of Heat in Solids*, Clarendon Press, 1992.
4. Munson, B.R., Okiishi, T.H., Huebsch, W.W., and Rothmayer, A.P., *Fluid Mechanics*, Singapore: Wiley, 2013.
5. Volterra, V., Note on the Application of the Method of Images to Problems of Vibrations, *Proc. Lond. Math. Soc*., 1905, vol. 2, no. 1, pp. 327–331.
6. Maxwell, J.C., *A Treatise on Electricity and Magnetism*. V. 1, Clarendon Press, 1873.
7. Eshelby, J.D., The Force on an Elastic Singularity, *Philos. Trans. Roy Soc. Lond. A. Math. Phys. Sci*., 1951, vol. 244, no. 877, pp. 87–112.
8. Head, A.K., The Interaction of Dislocations and Boundaries, *Philos. Mag. J. Sci*., 1953, vol. 44, no. 348, pp. 92–94.
9. Head, A.K., Edge Dislocations in Inhomogeneous Media, *Proc. Phys. Soc. B*, 1953, vol. 66, no. 9, p. 793.
10. Dundurs, J., Elastic Interaction of Dislocations with Inhomogeneities, in *Mathematical Theory of Dislocations*, 1969, pp. 70–115.
11. Taylor, R.I., The Force on a Screw Dislocation Due to a Series of Layers of Alternating Shear Modulus, *Semiconduct. Sci. Technol*., 1989, vol. 4, no. 8, p. 612.
12. Friedman, L.H. and Chrzan, D.C., Scaling Theory of the Hall–Petch Relation for Multilayers, *Phys. Rev. Lett*., 1998, vol. 81, no. 13, p. 2715.
13. Chou, Y.T., Pande, C.S., and Masumura, R.A., The Role of Harmonic Functions in Dislocation–Boundary Interactions by the Method of Images, *Mater. Sci. Eng. A*, 2007, vol. 452, pp. 99–102.
14. Ma, C.C. and Lu, H.T., Theoretical Analysis of Screw Dislocations and Image Forces in Anisotropic Multilayered Media, *Phys. Rev. B*, 2006, vol. 73, no. 14, p. 144102.
15. Wen, J. and Wu, M.S., Analysis of a Line Defect in a Multilayered Smart Structure by the Image Method, *Mech. Mater*., 2007, vol. 39, no. 2, pp. 126–144.
16. Zhou, K. and Wu, M.S., Elastic Fields Due to an Edge Dislocation in an Isotropic Film–Substrate by the Image Method, *Acta Mech*., 2010, vol. 211, no. 3–4, pp. 271–292.
17. Ogbonna, N., Force on a Screw Dislocation in a Multiphase Laminated Structure, *Math. Mech. Solids*, 2014, vol. 19, no. 6, pp. 694–702.
18. Ogbonna, N., On Screw Dislocation in a Multiphase Lamellar Inclusion, *J. Niger. Math. Soc*., 2015, vol. 34, no. 1, pp. 32–39.
19. Chou, T.W., Elastic Behavior of Disclinations in Nonhomogenous Media, *J. Appl. Phys*., 1971, vol. 42, no. 12, pp. 4931–4935.
20. Chou, T.W. and Pan, Y.C., Elastic Energies of Disclinations in Hexagonal Crystals, *J. Appl. Phys*., 1973, vol. 44, no. 1, pp. 63–65.
21. Eshelby, J.D., Screw Dislocations in Thin Rods, *J. Appl. Phys*., 1953, vol. 24, no. 2, pp. 176–179.
22. Ogbonna, N., On Elastic Interaction of a Screw Dislocation with a Coated Cylindrical Inclusion, *J. Eng. Math*., 2016, vol. 99, no. 1, pp. 203–212.
23. Wang, X. and Pan, E., Screw Dislocations in Piezoelectric Nanowires, *Mech. Res. Comm*., 2010, vol. 37, no. 8, pp. 707–711.
24. Dundurs, J. and Mura, T., Interaction between an Edge Dislocation and a Circular Inclusion, *J. Mech. Phys. Solids*, 1964, vol. 12, no. 3, pp. 177–189.
25. Dundurs, J. and Hetényi, M., The Elastic Plane with a Circular Insert, Loaded by a Radial Force, *J. Appl. Mech*., 1961, vol. 28, no. 1, p. 103.
26. Hetényi, M. and Dundurs, J., The Elastic Plane with a Circular Insert, Loaded by a Tangentially Directed Force, *J. Appl. Mech*., 1962, vol. 29, no. 2, p. 362.
27. List, R.D., A Two-Dimensional Circular Inclusion Problem, *Math. Proc. Cambridge Philos. Soc*., 1969, vol. 65, no. 3, pp. 823–830.
28. Povstenko, Yu.Z., Interaction between an Edge Dislocation and a Circular Boundary in the Presence of an Alien Surface Layer, *Sov. Appl. Mech*., 1975, vol. 11, no. 3, pp. 272–277.
29. Fukuzaki, K. and Shioya, S., On the Interaction between an Edge Dislocation and Two Circular Inclusions in an Infinite Medium, *Int. J. Eng. Sci*., 1986, vol. 24, no. 12, pp. 1771–1787.
30. Chen, D.H., Green's Functions for a Point Force and Dislocation Outside an Elliptic Inclusion in Plane Elasticity, *ZAMP*, 1996, vol. 47, no. 6, pp. 894–905.
31. Warren, W.E., The Edge Dislocation Inside an Elliptical Inclusion, *Mech. Mater*., 1983, vol. 2, no. 4, pp. 319–330.
32. Fang, Q.H., Liu, Y.W., and Jiang, C.P., Edge Dislocation Interacting with an Interfacial Crack Along a Circular Inhomogeneity, *Int. J. Solids Struct*., 2003, vol. 40, no. 21, pp. 5781–5797.
33. Wang, X., Interaction between an Edge Dislocation and a Circular Inclusion with an Inhomogeneously Imperfect Interface, *Mech. Res. Commun*., 2006, vol. 33, no. 1, pp. 17–25.

34. Dai, D.N., An Edge Dislocation Inside a Semi-Infinite Plane Containing a Circular Hole, *Int. J. Solids Struct*., 2018, vol. 136, pp. 295–305.
35. Malvern, L.E., *Introduction to the Mechanics of a Continuous*, Englewood Clifs, N.J.: Prentice-Hall, 1969.
36. Muskhelishvili N.I. *Some Basic Problems of the Mathematical Theory of Elasticity*, Graningen: Noordhoff, 1954.
37. Ardakani, S.M. and Ulm, F.J., Chemoelastic Fracture Mechanics Model for Cement Sheath Integrity, *J. Eng. Mech*., 2014, vol. 140, no. 4, p. 04013009.
38. Lardner, R.W., *Mathematical Theory of Dislocations and Fracture*, Toronto: University of Toronto Press, 1974.
39. Chen, Y.Z. and Lin, X.Y., Potentials In-Plane Elasticity by Distribution of Dislocation Doublet or Force Doublet Along a Curve, *Int. J. Eng. Sci*., 1998, vol. 36, no. 1, pp. 23–31.
40. Denda, M. and Kosaka, I., Dislocation and Point-Force-Based Approach to the Special Green's Function BEM for Elliptic Hole and Crack Problems in Two Dimensions, *Int. J. Numer. Meth. Eng*., 1997, vol. 40, no. 15, pp. 2857–2889.
41. Green, A.E. and Zerna, W., *Theoretical Elasticity*, New York: Dover Publications, 2012.